IEEE Access
Multidisciplinary : Rapid Review : Open Access Journal

Received March 5, 2020, accepted March 22, 2020, date of publication April 6, 2020, date of current version April 22, 2020.

Digital Object Identifier 10.1109/ACCESS.2020.2985776

Air-Core Ring Fiber With >1000 Radially Fundamental OAM Modes Across O, E, S, C, and L Bands

YINGNING WANG[1], CHANGJING BAO[2], WENPU GENG[1], YAO LU[1], YUXI FANG[1], BAIWEI MAO[1], YAN-GE LIU[1], BO LIU[1], HAO HUANG[2], YONGXIONG REN[2], ZHONGQI PAN[3], (Senior Member, IEEE), AND YANG YUE[1]

[1]Institute of Modern Optics, Nankai University, Tianjin 300350, China
[2]Department of Electrical Engineering, University of Southern California, Los Angeles, CA 90089, USA
[3]Department of Electrical and Computer Engineering, University of Louisiana at Lafayette, Lafayette, LA 70504, USA

Corresponding author: Yang Yue (yueyang@nankai.edu.cn)

This work was supported in part by the National Key Research and Development Program of China under Grant 2018YFB0703500 and Grant 2018YFB0504400, in part by the National Natural Science Foundation of China (NSFC) under Grant 11774181 and Grant 61775107, and in part by the Fundamental Research Funds for the Central Universities, Nankai University, under Grant 63191511.

ABSTRACT In this work, an air-core ring fiber is designed with a record high 1322 orbital angular momentum (OAM) modes at 1550 nm while maintaining radially single-mode condition. Moreover, it can support over 1004 OAM modes across all O, E, S, C, and L bands, exploiting to our knowledge the highest number of OAM modes ever supported in the optical fiber within a wide wavelength range. Simulations show that, across the C and L bands, the fiber with 55-μm air-core radius and 0.45-μm ring width can preserve 3.3×10^{-3} effective refraction index difference between the two highest-order OAM modes $HE_{340,1}$ and $EH_{271,1}$. This enables efficient mode separation, and thus achieving stable OAM modes transmission. The effective refractive index differences between the even and odd fiber eigenmodes are also analyzed in the elliptical and bent fibers. We note that higher-order OAM modes are more tolerant to the fiber ellipticity and bending. This ring fiber design has the potential to increase the spectral efficiency and the overall capacity in fiber-based communications system.

INDEX TERMS Orbital angular momentum, fiber optics, ring fiber, multiplexing.

I. INTRODUCTION

Acritical issue of the optical fiber communications society is to meet the ever-growing requirement on data transmission capacity. Research and industrial development efforts have been utilizing multiplexing technology through different dimensions of photon, such as time, wavelength, amplitude, phase, polarization, and space, to significantly increase the capacity over the past few decades [1]. For example, as the most popular and mature dimension, hundreds of data-capacity increments can be achieved with wavelength-division multiplexing (WDM) [2]. During the past decade, coherent technology has been extensively developed and implemented by the optical fiber communications industry. By utilizing the dimensions of the polarization, amplitude, and phase, this technology can significantly increase the spectral efficiency thus the overall data rate and capacity [3]. Fueled by emerging bandwidth-hungry applications, another dimension of photon has recently gained much attention in optical communications. Different fiber modes are being investigated to carry independent data streams, which can be spatial linearly polarized (LP) modes or orbital angular momentum (OAM) modes [4], [5].

OAM has enabled a variety of applications, such as micro-manipulation [6], [7], imaging [8], [9], and sensing [10], [11]. The distinguishing feature of an OAM beam is that it has the helical phase front named as exp $(il\theta)$ and discrete value of $l\eta$ per photon, where θ refers to the azimuthal angle and η is Plank's constant. l is an unlimited value in theory termed as the topological charge number, thus, the quantity of OAM-carrying beams is infinite in principle. Since coaxially light beams with different OAM states can be efficiently

The associate editor coordinating the review of this manuscript and approving it for publication was Tianhua Xu.

separated, it is possible to increase the spectral efficiency and data capacity of communication systems by multiplexing and demultiplexing the OAM modes [12]–[14].

Due to the unique OAM mode shape, ring-shaped high-index fiber is widely used for OAM-based fiber devices and communications systems [15], [16]. The ring fiber's annular shape profile makes it suitable for preserving OAM modes, as the OAM beams also has a ring-shaped intensity profile. With proper fiber parameter choice, maintaining the radially fundamental mode condition could potentially reduce the mode crosstalk and simplify the processes of multiplexing and demultiplexing [17]–[20]. One pioneer research has shown the capability of transmitting 1.6-Tb/s data-carrying OAM modes over 1.1-km ring fiber without using multiple-input and multiple-output (MIMO) technology [5]. Another latest research shows the aggregated capacity of 2.56-Tb/s data-carrying 8-OAM modes over 50-km specially designed ring-core fiber, using only modular 4×4 MIMO equalization [21]. Recently, air core ring fiber has been proposed and experimentally demonstrated [22]–[26], which enhanced the stability for OAM modes [27]. Due to its improved index contrast between the high-index ring and air core regions, more OAM modes can thus be supported. Latest study showed that 32 OAM modes can be supported in a single-ring fiber [28]. By further using the multi-core fiber concept, multi-ring micro-structured fiber was designed to support up to 646 OAM modes in the C band [29]. A laudable goal would be to enhance the index contrast among core, ring, and cladding regions, to further increase the number of supported OAM modes.

In this paper, we propose and design an air-core fiber with a single As_2S_3 high-index ring. Due to the large index-contrast among the low-index air core, high-index As_2S_3 ring, and the SiO_2 cladding, this structure can support a record high number of OAM modes in a single fiber. By adjusting the fiber structure, including the air-core and the ring width, we study the influence of the different fiber parameters on the total supported OAM mode number. According to the results, the hollow silica fiber with a 55-μm air core and a 0.45-μm thickness of As_2S_3 ring is designed to support fiber eigenmodes up to $HE_{365,1}$ and $EH_{297,1}$. This provides 1322 OAM modes at 1550 nm while maintaining single radial mode condition. In another design, a hollow silica fiber with a 55-μm air core and a 0.35-μm thickness of As_2S_3 ring, can support more than 1004 OAM modes from 1260 nm to 1625 nm, covering O, E, S, C, and L bands. It is the highest number of OAM modes ever supported in an optical fiber to the best of our knowledge.

II. CONCEPT AND FIBER STRUCTURE

Figure 1 illustrates the concept of OAM mode multiplexing into air-core As_2S_3 ring fiber, in which the OAM modes with different l states can be transmitted simultaneously. Here, we propose a specially designed fiber with an air-core and a high-index As_2S_3 ring region to better guide the OAM modes. The cross section of the designed ring fiber is also

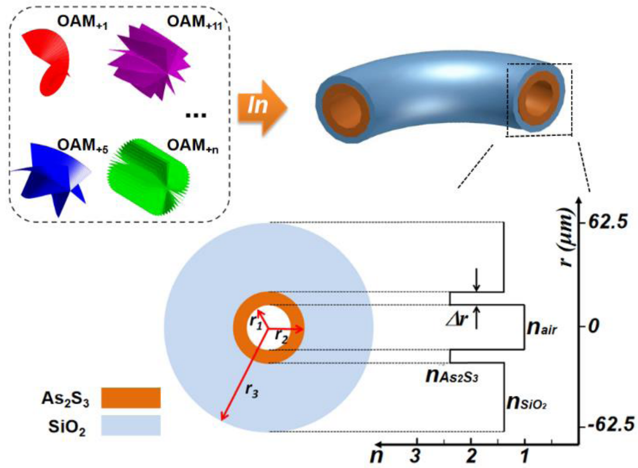

FIGURE 1. Concept of OAM mode multiplexing and cross-section of the air-core As_2S_3 ring fiber.

shown in Figure 1. To increase the refractive index contrast between different fiber materials, a hollow air-core is thus chosen for a lowest possible refractive index 1. Furthermore, we select As_2S_3 ($n = 2.4373$ at 1550 nm) and SiO_2 ($n = 1.4440$ at 1550 nm) as the materials of the ring region and cladding regions to achieve large index contrast. The ring-core fiber design increases the mode effective refractive index difference, and thus significantly reduces the intermodal coupling. The large material index-contrast among the cladding, the core, and the ring region enables a large effective-index separation among the $HE_{l+1,1}$ or $EH_{l-1,1}$ mode of the same $|l|$ family, which potentially reduces the modal crosstalk and facilitates stable transmission of OAM modes. This structure design and material choice is feasible, as chalcogenide thin-film fibers have been manufactured in practice [30], [31]. According to the As_2S_3 material loss [32], the optical loss is several times larger than 0.03 dB/m at 1550 nm. Furthermore, previous experiment result has shown that relatively low loss 0.012 dB/m at 3000 nm and 0.014 dB/m at 4800 nm can be achieved in As_2S_3 multimode fibers. Moreover, the fabrication of this air-core ring fiber can be realized via modified chemical vapor deposition (MCVD) [25], [28], where the hollow core diameter is controlled during the fiber drawing process to achieve the target value. The deposited As_2S_3 region is relatively thin, so that only the radially fundamental modes are supported, which can make the multiplexing and demultiplexing of the OAM modes easier and results in a good mode separation. Moreover, we choose a 125-μm fiber cladding diameter, the same as the standard single-mode optical fiber (SMF).

III. MODE PROPERTY

In Figure 2(a) one can see that the simulated distributions of the normalized intensity and the phase for $OAM_{l,1}$ modes ($|l| = 1, 2, 4, 6, 8$) in the fiber ($r_1 = 1$ μm, $\Delta r = 0.45$ μm), which are composed by the even and odd eigenmodes. The upper color bar stands for the intensity level of the

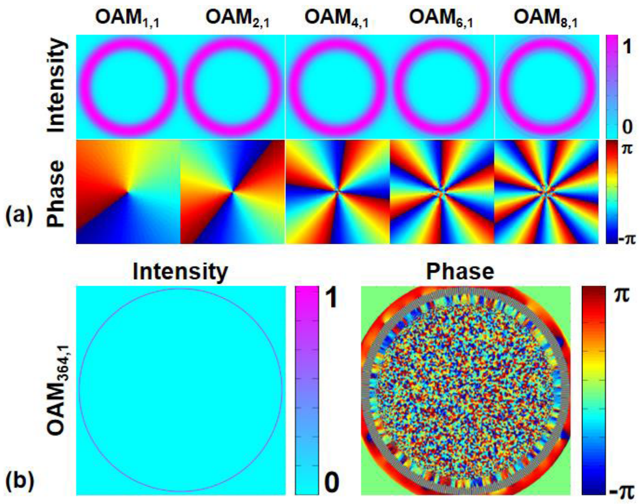

FIGURE 2. (a) The normalized intensity and phase distribution of the supported OAM modes in the air-core As_2S_3 ring fiber ($r_1 = 1\ \mu m$, $\Delta r = 0.45\ \mu m$). (b) The normalized intensity and phase distribution of the $OAM_{364,1}$ mode in the air-core As_2S_3 ring fiber ($r_1 = 55\ \mu m$, $\Delta r = 0.45\ \mu m$).

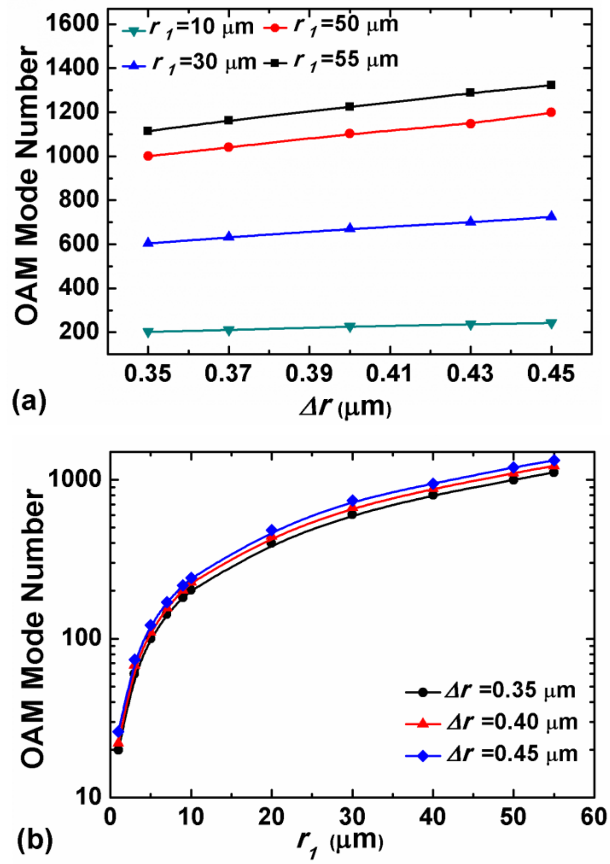

FIGURE 3. (a) OAM mode number supported in the air-core ring fiber as a function of the ring width (Δr) with different air-core radii (r_1). (b) OAM mode number supported in the air-core ring fiber as a function of the air-core radius (r_1) with different ring widths (Δr).

normalized field strength of the OAM modes, while the bottom color bar represents the phase change of the OAM modes. The profiles indicate that the OAM modes still remain the shape of the ring-like intensity distribution and the phase distribution of the OAM_l, 1 mode shows a $2l\pi$ phase change azimuthally. Besides, the intensity and phase distributions of the $OAM_{364,1}$ mode ($OAM_l-1,1 = HE^{even}_{l,1} + i\times HE^{odd}_{l,1}$, $l = 365$) which is the maximum supported OAM mode at 1550 nm is depicted in figure 2(b) for the designed fiber with $r_1 = 55\ \mu m$ and $\Delta r = 0.45\ \mu m$.

In the following, we further investigate the OAM mode number variations in the designed air-core As_2S_3 ring fiber with different ring widths (Δr) and air-core radii (r_1) by using full-vector finite-element-method (FEM). We first study the OAM mode number (composed by $HE^{even}_{m,1} + i\times HE^{odd}_{m,1}$ or $EH^{even}_{n,1} + i\times EH^{odd}_{n,1}$) that can be supported in the fiber with different air-core radii. The previous researches have shown that maintaining the radially fundamental mode condition can help avoid the modal crosstalk between the OAM modes of the first radial order and the higher radial order OAM modes. And we find that the ring width should be kept less than 0.45 μm to maintain the radially single-mode condition. As shown in Figure 3(a), the supported OAM mode number increases gradually with ring widths which could be explained that the fiber with larger ring width has more radial space. Then we further investigate the OAM number supported in the fiber with different air-core radii as shown in Figure 3(b) and we note that the supported OAM mode number increases 50 times from 20 to approximately 1000 with r_1 from 1 to 55 μm, which is due to the increased azimuthal space. The air-core ring fiber with $r_1 = 55\ \mu m$ and $\Delta r = 0.45\ \mu m$ can support 1322 OAM modes at 1550 nm, in which the highest order eigenmodes are $HE_{365,1}$ and $EH_{297,1}$ respectively. Thus, enlarging the core radius is a more efficient way to increase the supported OAM mode numbers.

Figure 4 illustrates the supported OAM mode number as a function of wavelength with different ring widths, in which the solid line means maintaining the radially single-mode

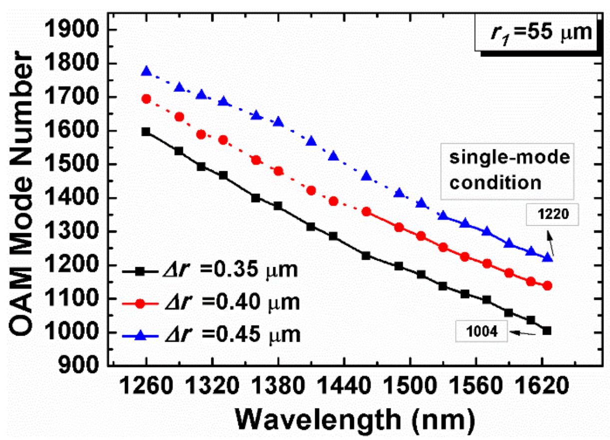

FIGURE 4. OAM mode number of the air-core ring fiber with $r_1 = 55\ \mu m$ as a function of wavelength with different ring widths (Δr).

condition and the dot line means that radially high-order mode appears. The radially single-mode condition starts from 1460 nm and 1530 nm for $\Delta r = 0.4\ \mu$m and $\Delta r = 0.45\ \mu$m, respectively. One can see that approximately 1000 OAM modes can be supported over a broad wavelength range, while maintaining the radially fundamental mode condition. Larger Δr gives more supported OAM modes at a certain wavelength, but radially high-order mode will appear from a shorter wavelength. The designed air-core ring fiber ($r_1 = 55\ \mu$m, $\Delta r = 0.45\ \mu$m) can support more than 1220 OAM modes across C and L bands (from 1530 nm to 1625 nm), while more than 1004 can be transmitted across O, E, S, C, and L-band (from 1260 nm to 1625 nm) using the designed fiber with $r_1 = 55\ \mu$m and $\Delta r = 0.35\ \mu$m. The fiber with larger Δr can support more OAM modes, but with sacrificed single-mode operating range. Consequently, there is a trade-off between the single-mode condition bandwidth and the supported mode numbers. This provides and effective manner for increasing the transmission capacity by using more WDM channels.

Figure 5 (a) illustrates the effective refractive indices (n_{eff}) of some OAM modes supported in the fiber as a function of wavelength with fiber parameters of $r_1 = 55\ \mu$m and $\Delta r = 0.45\ \mu$m. One can see that the effective refractive indices of the modes decrease as the wavelength increases and the maximum modes of HE and EH supported by the fiber across C and L bands can be up to $HE_{340,1}$ and $EH_{271,1}$, respectively. A number of the previous researches have suggested that the effective index difference between the adjacent modes should be maintained above 10^{-4} to assure the good separation and avoid the crosstalk [28]. According to the simulation, the refractive index difference of the nearest-neighbor fiber eigenmodes rises up with the mode order. According to the simulation, the effective index differences of the few adjacent low-order eigenmodes are unable to separate enough, but for the most eigenmodes, the condition is achievable. Besides, the effective index difference between $HE_{340,1}$ and $EH_{271,1}$ reaches to approximately 3.3×10^{-3}, which can achieve the stable transmission of OAM modes at 1550 nm. Moreover, the simulation result shows that the $EH_{1,1}$ mode turns out after more than 150 *HE* modes as shown in the Figure 5 (a), which can be explained with the fact that the high index contrast between the air-core and the ring leads to the larger index difference. The relatively large effective index differences between $HE_{l+1,1}$ and $EH_{l-1,1}$ can avoid them to be degenerated into *LP* modes.

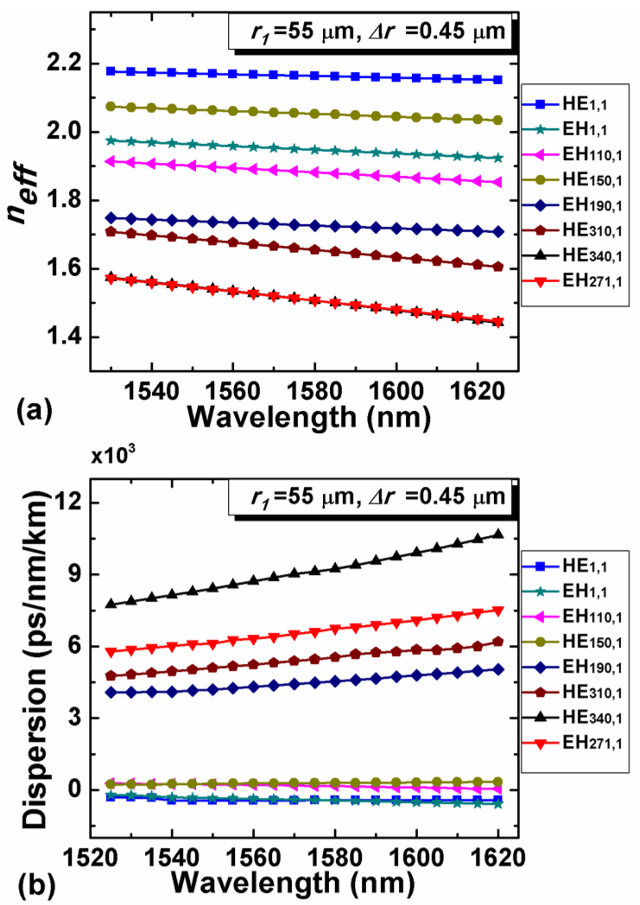

FIGURE 5. **(a) Effective refractive index and (b) dispersion of the air-core fiber with parameters of $r_1 = 55\ \mu$m and $\Delta r = 0.45\ \mu$m as a function of wavelength for different vortex modes.**

Figure 5 (b) shows the dispersion characteristics of the eigenmodes that form OAM modes in the corresponding structure of the fiber. As seen in the figure, the chromatic dispersion increased from -442.23 to more than 8000 ps/nm/km as the mode order becomes higher at 1550 nm. The value of dispersion is larger than traditional fiber due to the As_2S_3 material dispersion. Noted that although the dispersions of the high-order modes are very large, OAM dispersion compensating fiber (DCF) with large negative dispersion can be potentially used to compensate them [14]. Furthermore, chromatic dispersion can also be compensated by the digital signal processing (DSP) in the coherent optical communications systems [33].

IV. FIBER ELLIPTICITY AND BENDING

Strain, stress, twist and other perturbations imposed on the ring fiber may lead to fiber deformed (i.e. ellipticity and bending), inducing polarization mode dispersion (PMD) and birefringence. Moreover, the OAM modes are made up of two fiber eigenmodes, in which the even and odd modes of $\text{HE}_{m,1}$ or $\text{EH}_{n,1}$ with a $\pm\pi/2$ phase shift compound an OAM mode, thus, the fiber ellipticity and bending can also make a difference in the mode profile and purity of OAM modes as they can bring differences to the two fiber eigenmodes' propagation constants.

In the following, by fixing the wavelength at 1550 nm, we further research the influence on the property of the OAM modes while the high-index ring region has nonperfect circularity (ellipticity) or the fiber bends. We find that the fiber ellipticity and bending have most significant impact on the effective refractive indices of the $EH_{1,1}$ mode and $HE_{1,1}$ mode, respectively. Figure 6(a) illustrates the effective refractive index difference (Δn_{eff}) between the even and odd fiber eigenmodes of $EH_{1,1}$ as a function of the ellipticity of fiber with different air-core radii (r_1). The simulation results show that the fiber ellipticity has less impact on the fiber with larger inner radius. Figure 6(b) illustrates the effective refractive index difference between the even and odd fiber eigenmodes of $HE_{1,1}$ as a function of the fiber bend radius with different ring's inner radii. In contrast to the fiber ellipticity, the simulation shows that the smaller inner radius, the higher tolerance to the fiber bend radius. In sum, the designed fiber with larger air-core radius is more tolerant to ellipticity and more sensitive to the fiber bending, thus, we should choose proper air-core radius according to different applications.

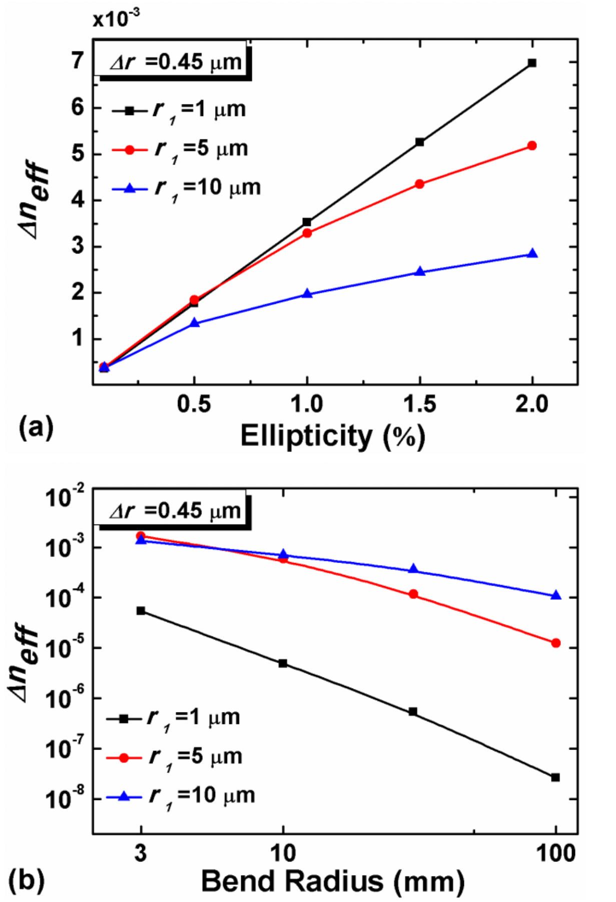

FIGURE 6. (a) The effective refractive indices of fiber eigenmodes of $EH_{1,1}$ as a function of the fiber ellipticity with different air-core radii (r_1). (b) the effective refractive indices of fiber eigenmodes of $HE_{1,1}$ as a function of the fiber bend radius with different air-core radii (r_1).

Figure 7(a) shows the effective refractive index difference between the even and odd fiber eigenmodes as a function of the fiber ellipticity with $r_1 = 10\ \mu m$ and $\Delta r = 0.45\ \mu m$. The profile and purity of the OAM mode can be degraded by the effective refractive index difference between the even and odd fiber eigenmodes which is caused by the fiber ellipticity and fiber bending. We note that the high-order OAM modes (composed by the even and odd modes of $HE_{32,1}$, $EH_{30,1}$,

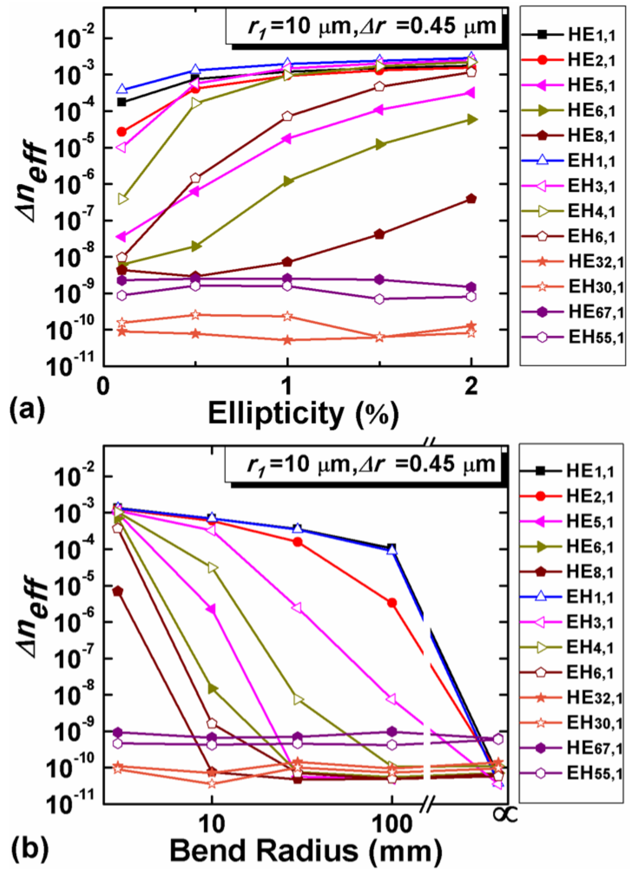

FIGURE 7. The effective refractive indices of the OAM modes in the air-core ring fiber with $r_1 = 10\ \mu m$ and $\Delta r = 0.45\ \mu m$ as functions of (a) fiber ellipticity and (b) fiber bend radius.

$HE_{67,1}$, $EH_{55,1}$) have stronger tolerance to the fiber ellipticity than that of the low-order eigenmodes (composed by the even and odd modes of $HE_{2,1}$, $HE_{5,1}$, $EH_{1,1}$, $HE_{6,1}$, $EH_{3,1}$, $EH_{4,1}$). This is because that the high-order OAM modes have more azimuthal periods in their transverse field distribution, which could mitigate the effect from fiber ellipticity. For low-order modes, with the increase of the ellipticity, the effective refractive index difference between the even and odd fiber eigenmodes also increases. As the air-core ring fiber has 2% ellipticity, the maximum effective refractive index difference of the $EH_{1,1}$ mode is approximately 2.84×10^{-3}. For high-order OAM modes, the simulation results show that all the effective refractive index differences between the even and odd fiber eigenmodes are around 1×10^{-10}.

Figure 7(b) shows the effective refractive index difference between the even and odd fiber eigenmodes as a function of the fiber bend radius. One can see that for low-order modes, the effective refractive index difference between the even and odd fiber eigenmodes increases as reducing the bend radius from 100 to 3 mm, while the high-order OAM modes show more tolerance to the fiber bending. This can also be explained that the high-order OAM modes have more azimuthal periods, thus, they are more stable as the fiber

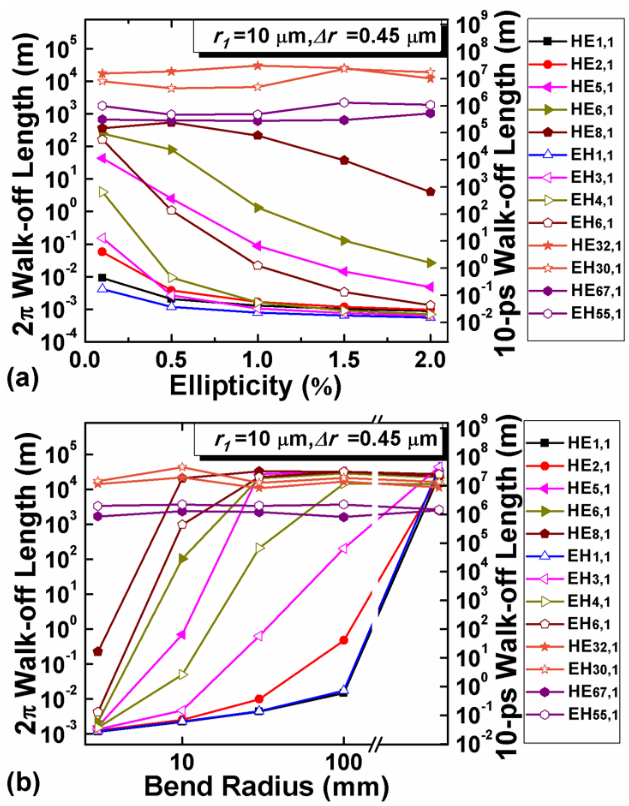

FIGURE 8. 2π walk-off length and 10-ps walk-off length for different OAM modes in the air-core ring fiber with $r_1 = 10$ μm and $\Delta r = 0.45$ μm as functions of (a) fiber ellipticity and (b) fiber bend radius.

becomes deformed. The maximum effective refractive index difference for the $HE_{1,1}$ is 1.34×10^{-3} as the fiber has 3-mm bend radius.

The ellipticity and bending of the fiber cause the effective refractive index difference between the even and odd fiber eigenmodes that forms an OAM mode. Such effective refractive index difference can affect the temporal walk-off effect upon propagation. Figure 8 (a) and (b) depict the walk-off length variations for different OAM modes in the air-core ring fiber with $r_1 = 10$ μm and $\Delta r = 0.45$ μm as functions of fiber ellipticity and bend radius with $r_1 = 10$ μm and $\Delta r = 0.45$ μm. Here, we use two parameters, 2π walk-off length ($L_{2\pi}$) and 10-ps walk-off length (L_{10ps}), to describe the intra-mode walk-off of the OAM modes in a deformed fiber. They can be expressed as

$$L_{2\pi} = \frac{\lambda}{n_{eff}^{even} - n_{eff}^{odd}} \quad (1)$$

$$L_{10_{ps}} = \frac{c \times \Delta t}{n_{eff}^{even} - n_{eff}^{odd}} \quad (2)$$

where λ is the wavelength, c and Δt are the light velocity in vacuum and the temporal walk off time, respectively. [18], [19]. Moreover, n_{eff}^{even} and n_{eff}^{odd} are the effective refractive indices of the even and odd eigenmodes, respectively. We note that the high-order OAM modes show longer 2π walk-off length and 10-ps walk-off length than that of the low-order OAM modes. Moreover, for the low-order OAM modes, as the fiber ellipticity becomes larger or the fiber bend radius becomes smaller, both 2π walk-off length and 10-ps walk-off length decrease.

ACKNOWLEDGMENT

(Yingning Wang and Changjing Bao contributed equally to this work.)

REFERENCES

[1] P. J. Winzer, "Modulation and multiplexing in optical communications," in *Proc. Conf. Lasers Electro-Opt./Int. Quantum Electron. Conf.*, Baltimore, MD, USA, 2009, pp. 1–2.

[2] S. Okamoto, K. Horikoshi, F. Hamaoka, K. Minoguchi, and A. Hirano, "5-band (O, E, S, C, and L) WDM transmission with wavelength adaptive modulation format allocation," in *Proc. Eur. Conf. Opt. Commun.*, Düsseldorf, Germany, 2016, pp. 1–3.

[3] B. J. Puttnam, G. Rademacher, R. S. Luís, T. A. Eriksson, W. Klaus, Y. Awaji, N. Wada, K. Maeda, S. Takasaka, and R. Sugizaki, "0.715 Pb/s transmission over 2,009.6 km in 19-core cladding pumped EDFA amplified MCF link," in *Proc. Opt. Fiber Commun. Conf. Postdeadline Papers*, 2019, Paper Th4B.1.

[4] R. G. H. van Uden, R. A. Correa, E. A. Lopez, F. M. Huijskens, C. Xia, G. Li, A. Schülzgen, H. de Waardt, A. M. J. Koonen, and C. M. Okonkwo, "Ultra-high-density spatial division multiplexing with a few-mode multicore fibre," *Nature Photon.*, vol. 8, no. 11, pp. 865–870, Nov. 2014.

[5] N. Bozinovic, Y. Yue, Y. Ren, M. Tur, P. Kristensen, H. Huang, A. E. Willner, and S. Ramachandran, "Terabit-scale orbital angular momentum mode division multiplexing in fibers," *Science*, vol. 340, no. 6140, pp. 1545–1548, Jun. 2013.

[6] M. E. J. Friese, T. A. Nieminen, N. R. Heckenberg, and H. Rubinsztein-Dunlop, "Optical alignment and spinning of laser-trapped microscopic particles," *Nature*, vol. 394, no. 6691, pp. 348–350, Jul. 1998.

[7] K. Dholakia and T. Čižmár, "Shaping the future of manipulation," *Nature Photon.*, vol. 5, no. 6, pp. 335–342, Jun. 2011.

[8] A. Jesacher, M. Ritsch-Marte, and R. Piestun, "Three-dimensional information from two-dimensional scans: A scanning microscope with postacquisition refocusing capability," *Optica*, vol. 2, no. 3, p. 210, Mar. 2015.

[9] G. A. Swartzlander, E. L. Ford, R. S. Abdul-Malik, L. M. Close, M. A. Peters, D. M. Palacios, and D. W. Wilson, "Astronomical demonstration of an optical vortex coronagraph," *Opt. Express*, vol. 16, no. 14, pp. 10200–10207, 2008.

[10] N. Cvijetic, G. Milione, E. Ip, and T. Wang, "Detecting lateral motion using Light's orbital angular momentum," *Sci. Rep.*, vol. 5, no. 1, Dec. 2015, Art. no. 15422.

[11] G. Xie, H. Song, Z. Zhao, G. Milione, Y. Ren, C. Liu, R. Zhang, C. Bao, L. Li, Z. Wang, K. Pang, D. Starodubov, B. Lynn, M. Tur, and A. E. Willner, "Using a complex optical orbital-angular-momentum spectrum to measure object parameters," *Opt. Lett.*, vol. 42, no. 21, pp. 4482–4485, Nov. 2017.

[12] A. E. Willner, H. Huang, Y. Yan, Y. Ren, N. Ahmed, G. Xie, C. Bao, L. Li, Y. Cao, Z. Zhao, J. Wang, M. P. J. Lavery, M. Tur, S. Ramachandran, A. F. Molisch, N. Ashrafi, and S. Ashrafi, "Optical communications using orbital angular momentum beams," *Adv. Opt. Photon.*, vol. 7, pp. 66–106, Mar. 2015.

[13] A. Trichili, K.-H. Park, M. Zghal, B. S. Ooi, and M.-S. Alouini, "Communicating using spatial mode multiplexing: Potentials, challenges, and perspectives," *IEEE Commun. Surveys Tuts.*, vol. 21, no. 4, pp. 3175–3203, May 2019.

[14] Z.-A. Hu, Y.-Q. Huang, A.-P. Luo, H. Cui, Z.-C. Luo, and W.-C. Xu, "Photonic crystal fiber for supporting 26 orbital angular momentum modes," *Opt. Express*, vol. 24, no. 15, pp. 17285–17291, Jul. 2016.

[15] Q. Kang, P. Gregg, Y. Jung, E. L. Lim, S.-U. Alam, S. Ramachandran, and D. J. Richardson, "Amplification of 12 OAM modes in an air-core erbium doped fiber," *Opt. Express*, vol. 23, no. 22, pp. 28341–28348, Nov. 2015.

[16] G. Zhu, Z. Hu, X. Wu, C. Du, W. Luo, Y. Chen, X. Cai, J. Liu, J. Zhu, and S. Yu, "Scalable mode division multiplexed transmission over a 10-km ring-core fiber using high-order orbital angular momentum modes," *Opt. Express*, vol. 26, no. 2, p. 594, Jan. 2018.

[17] K. Ingerslev, P. Gregg, M. Galili, F. Da Ros, H. Hu, F. Bao, M. A. U. Castaneda, P. Kristensen, A. Rubano, L. Marrucci, K. Rottwitt, T. Morioka, S. Ramachandran, and L. K. Oxenløwe, ''12 mode, WDM, MIMO-free orbital angular momentum transmission,'' *Opt. Express*, vol. 26, no. 16, pp. 20225–20232, Aug. 2018.
[18] L. Zhu, G. Zhu, A. Wang, L. Wang, J. Ai, S. Chen, C. Du, J. Liu, S. Yu, and J. Wang, ''18 km low-crosstalk OAM + WDM transmission with 224 individual channels enabled by a ring-core fiber with large high-order mode group separation,'' *Opt. Lett.*, vol. 43, no. 8, p. 1890, Apr. 2018.
[19] Y. Yue, Y. Yan, N. Ahmed, J.-Y. Yang, L. Zhang, Y. Ren, H. Huang, K. M. Birnbaum, B. I. Erkmen, S. Dolinar, M. Tur, and A. E. Willner, ''Mode properties and propagation effects of optical orbital angular momentum (OAM) modes in a ring fiber,'' *IEEE Photon. J.*, vol. 4, no. 2, pp. 535–543, Apr. 2012.
[20] S. Li and J. Wang, ''A compact trench-assisted multi-orbital-angular-momentum multi-ring fiber for ultrahigh-density space-division multiplexing (19 rings × 22 Modes),'' *Sci. Rep.*, vol. 4, no. 1, May 2015, Art. no. 3853.
[21] J. Zhang, Y. Wen, H. Tan, J. Liu, L. Shen, M. Wang, J. Zhu, C. Guo, Y. Chen, Z. Li, and S. Yu, ''80-channel WDM-MDM transmission over 50-km ring-core fiber using a compact OAM DEMUX and modular 4×4 MIMO equalization,'' in *Proc. Opt. Fiber Commun. Conf. (OFC)*, 2019, pp. 1–3, Paper W3F.3.
[22] P. Gregg, P. Kristensen, A. Rubano, S. Golowich, L. Marrucci, and S. Ramachandran, ''Enhanced spin orbit interaction of light in highly confining optical fibers for mode division multiplexing,'' *Nature Commun.*, vol. 10, no. 1, p. 4707, Dec. 2019.
[23] Y. Peng, H. Jia, and L. Fang, ''Theoretical analysis of hollow ring-core optical fibre for transmitting orbital angular momentum modes,'' *J. Modern Opt.*, vol. 64, no. 18, pp. 1818–1832, Oct. 2017.
[24] P. Gregg, P. Kristensen, and S. Ramachandran, ''134 km OAM state propagation by recirculating fiber loop,'' *Opt. Express*, vol. 24, no. 17, pp. 18938–18947, Aug. 2016.
[25] P. Gregg, P. Kristensen, and S. Ramachandran, ''Conservation of orbital angular momentum in air-core optical fibers,'' *Optica*, vol. 2, no. 3, pp. 267–270, Mar. 2015.
[26] L. Liu, Q. Zhu, X. Sun, Y. Geng, W. Wang, W. Huang, X. Feng, and Y. Zhang, ''Edge-dip air core fiber for improvement of the transmission of higher-order OAM modes,'' *Proc. SPIE*, vol. 10710, Mar. 2018, Art. no. 107103E.
[27] S. Ramachandran, P. Gregg, P. Kristensen, and S. E. Golowich, ''On the scalability of ring fiber designs for OAM multiplexing,'' *Opt. Express*, vol. 23, no. 3, pp. 3721–3730, Feb. 2015.
[28] C. Brunet, P. Vaity, Y. Messaddeq, S. LaRochelle, and L. A. Rusch, ''Design, fabrication and validation of an OAM fiber supporting 36 states,'' *Opt. Express*, vol. 22, no. 21, pp. 26117–26127, Oct. 2014.
[29] C. Chen, G. Zhou, G. Zhou, M. Xu, Z. Hou, C. Xia, and J. Yuan, ''A multi-orbital-angular-momentum multi-ring micro-structured fiber with ultra-high-density and low-level crosstalk,'' *Opt. Commun.*, vol. 368, pp. 27–33, Jun. 2016.
[30] C. Markos, I. Kubat, and O. Bang, ''Hybrid polymer photonic crystal fiber with integrated chalcogenide glass nanofilms,'' *Sci. Rep.*, vol. 4, no. 1, May 2015, Art. no. 6057.
[31] C. Markos and C. R. R. Petersen, ''Multimaterial photonic crystal fibers,'' *Proc. SPIE*, vol. 10528, Feb. 2018, Art. no. 105280V.
[32] M. F. Churbanov, G. E. Snopatin, V. S. Shiryaev, V. G. Plotnichenko, and E. M. Dianov, ''Recent advances in preparation of high-purity glasses based on arsenic chalcogenides for fiber optics,'' *J. Non-Crystalline Solids*, vol. 357, nos. 11–13, pp. 2352–2357, Jun. 2011.
[33] T. Xu, G. Jacobsen, S. Popov, J. Li, E. Vanin, K. Wang, A. T. Friberg, and Y. Zhang, ''Chromatic dispersion compensation in coherent transmission system using digital filters,'' *Opt. Express*, vol. 18, no. 15, pp. 16243–16257, Jul. 2010.

YINGNING WANG received the B.S. degree in electronic science and technology from Shandong University, Qingdao, Shandong, China, in 2019. She is currently pursuing the M.S. degree in optical engineering with the Institute of Modern Optics, Nankai University, Tianjin, China.

CHANGJING BAO received the Ph.D. degree in electrical engineering from the University of Southern California, Los Angeles, CA, USA, in 2017. He has authored or coauthored more than 100 journal articles and conference proceedings. His research interests include optical communications, nonlinear optics, and integrated optics.

WENPU GENG received the B.S. degree in optical information science and technology from Nankai University, Tianjin, China, in 2019, where she is currently pursuing the M.S. degree in optical engineering with the Institute of Modern Optics.

YAO LU received the B.S. degree in optical information science and technology from Nankai University, Tianjin, China, in 2019. She is currently pursuing the M.S. degree in optical engineering with the Institute of Applied Physics, Chinese Academy of Sciences University, Shanghai, China.

YUXI FANG received the bachelor's degree in optical information science and technology from Anhui University, Hefei, Anhui, China, in 2018. She is currently pursuing the master's degree with the Institute of Modern Optics, Nankai University, Tianjin, China. Her research interest includes integrated optics.

BAIWEI MAO received the B.S. degree in optical information science and technology from the South China University of Technology, Guangzhou, Guangdong, China, in 2017. He is currently pursuing the Ph.D. degree in optical engineering with the Institute of Modern Optics, Nankai University, Tianjin, China.

YAN-GE LIU received the M.S. degree in optics from Nankai University, Tianjin, China, in 1998, and the Ph.D. degree in optic engineering from Tianjin University, Tianjin, in 2001.

She is currently a Professor with the Institute of Modern Optics, Nankai University. She has published more than 130 peer-reviewed journal articles with total citations of more than 2000 times. Her research interests include micro/nanostructured optical fiber devices, optical fiber communication and sensing technology, and optical fiber lasers and amplifiers.

BO LIU received the Ph.D. degree in optics from Nankai University, Tianjin, China, in 2004. He is currently a Professor with the Institute of Modern Optics, Nankai University. His major research interests include fiber sensors, fiber-grating-based photonic devices, and interrogation systems.

HAO HUANG received the B.S. degree from Jilin University, Changchun, China, in 2006, the M.S. degree from the Beijing University of Posts and Telecommunications, Beijing, China, in 2009, and the Ph.D. degree in electrical engineering from the University of Southern California, Los Angeles, CA, USA, in 2014. He is currently working with Lumentum Operations LLC as a Hardware Engineer. He has coauthored more than 100 publications, including peer-reviewed journals and conference proceedings. His research area includes optical communication system and components, optical sensing systems, and digital signal processing. He is a member of the Optical Society of America (OSA).

YONGXIONG REN received the B.E. degree in communications engineering from the Beijing University of Posts and Telecommunications (BUPT), Beijing, China, in 2008, the M.S. degree in radio physics from Peking University (PKU), Beijing, in 2011, and the Ph.D. degree in electrical engineering from the University of Southern California (USC), Los Angeles, CA, in 2016.

He has authored or coauthored more than 130 research articles with a Google Scholar citation number of more than 5500. His publications include 57 peer-reviewed journal articles, 76 international conference proceedings, one book chapter, and three patents. His main research focuses include high-capacity free-space and fiber optical communications, millimeter-wave communications, space division multiplexing, orbital angular momentum multiplexing, atmospheric optics, and atmospheric turbulence compensation.

ZHONGQI PAN (Senior Member, IEEE) received the B.S. and M.S. degrees from Tsinghua University, China, and the Ph.D. degree from the University of Southern California, Los Angeles, all in electrical engineering.

He is currently a Professor with the Department of Electrical and Computer Engineering. He also holds BORSF Endowed Professorship in Electrical Engineering II, and BellSouth/BoRSF Endowed Professorship in Telecommunications. He has authored/coauthored 160 publications, including five book chapters and 18 invited presentations/articles. He also has five U.S. patents and one China patent. His researches are in the area of photonics, including photonic devices, fiber communications, wavelength-division-multiplexing (WDM) technologies, optical performance monitoring, coherent optical communications, space-division-multiplexing (SDM) technologies, and fiber sensor technologies. He is a Senior Member of OSA.

YANG YUE received the B.S. and M.S. degrees in electrical engineering and optics from Nankai University, Tianjin, China, in 2004 and 2007, respectively, and the Ph.D. degree in electrical engineering from the University of Southern California, Los Angeles, CA, USA, in 2012.

He is currently a Professor with the Institute of Modern Optics, Nankai University, Tianjin, China. He has published over 150 peer-reviewed journal papers and conference proceedings, three edited books, one book chapter, more than ten invited papers, more than 30 issued or pending patents, and more than 80 invited presentations. His current research interests include intelligent photonics, optical communications and networking, optical interconnect, detection, imaging and display technology, integrated photonics, free-space, and fiber optics.

Dr. Yue is a member of the IEEE Communications Society (ComSoc), IEEE Photonics Society (IPS), International Society for Optical Engineering (SPIE), Optical Society of America (OSA), and the Photonics Society of Chinese-American (PSC). He is an Editor Board member for three scientific journals. He also served as a Guest Editor for six journal special issues, a Committee Member and a Session Chair for approximately 30 international conferences, a reviewer for more than 50 prestigious journals, and a Reviewer for OSA Centennial Special Events Grant 2016.